Hybrid ZnO/GaN distributed Bragg reflectors grown by plasma-assisted molecular beam epitaxy

David Adolph, Reza R. Zamani, Kimberly A. Dick, and Tommy Ive

---

Hybrid ZnO/GaN distributed Bragg reflectors grown by plasma-assisted molecular beam epitaxy

David Adolph,[1,a] Reza R. Zamani,[2] Kimberly A. Dick,[2,3] and Tommy Ive[1]

[1]*Department of Microtechnology and Nanoscience, Chalmers University of Technology, 41296 Gothenburg, Sweden*
[2]*Solid State Physics, Lund University, Box 118, S-22100 Lund, Sweden*
[3]*Centre for Analysis and Synthesis, Lund University, Box 124, 22100 Lund, Sweden*

We demonstrate crack-free ZnO/GaN distributed Bragg reflectors (DBRs) grown by hybrid plasma-assisted molecular beam epitaxy using the same growth chamber for continuous growth of both ZnO and GaN without exposure to air. This is the first time these ZnO/GaN DBRs have been demonstrated. The Bragg reflectors consisted up to 20 periods as shown with cross-sectional transmission electron microscopy. The maximum achieved reflectance was 77% with a 32 nm wide stopband centered at 500 nm. Growth along both (0001) and (000$\bar{1}$) directions was investigated. Low-temperature growth as well as two-step low/high-temperature deposition was carried out where the latter method improved the DBR reflectance. Samples grown along the (0001) direction yielded a better surface morphology as revealed by scanning electron microscopy and atomic force microscopy. Reciprocal space maps showed that ZnO(000$\bar{1}$)/GaN reflectors are relaxed whereas the ZnO(0001)/GaN DBRs are strained. The ability to n-type dope ZnO and GaN makes the ZnO(0001)/GaN DBRs interesting for various optoelectronic cavity structures. © 2016 Author(s). All article content, except where otherwise noted, is licensed under a Creative Commons Attribution (CC BY) license (http://creativecommons.org/licenses/by/4.0/). [http://dx.doi.org/10.1063/1.4960619]

Blue-emitting electrically injected vertical-cavity surface emitting lasers (VCSELs) based on GaN and related compounds have now been demonstrated by little more than a handful research groups.[1–6] Distributed Bragg reflectors (DBRs) are essential for the formation of the VCSEL optical cavity. In the literature, one can find two different approaches concerning the fabrication of the optical cavity.

The first approach relies on the epitaxial growth of a nitride-based ($Al_xGa_{1-x}N/Al_yGa_{1-y}N$, $Al_xGa_{1-x}N/GaN$, or AlInN/GaN) bottom DBR followed by the growth of the active region. A top dielectric DBR is then bonded externally which concludes the VCSEL optical structure.[2,3,7–9] This method has the advantage of simplifying the processing required for the fabrication of the VC-SEL device. However, the relatively small difference between the refractive index of $Al_xGa_{1-x}N$ or AlInN and GaN means that a large number of periods N (N > 20 for AlN/GaN and N > 40 for AlInN/GaN) is needed to achieve a high reflectance DBR. In the case of using $Al_xGa_{1-x}N$/GaN mirrors, strain-engineering is needed to avoid crack-formation due to the accumulation of tensile strain in the $Al_xGa_{1-x}N$ layers caused by the lattice-mismatch between high-Al containing $Al_xGa_{1-x}N$ and GaN.

The second approach involves epitaxial growth of the active region followed by lift-off to separate the active region from the substrate and flip-chip bonding where the active region is sequentially bonded to the top and bottom dielectric DBRs.[1,4–6,10–13] This method achieves high-reflectance mirrors with wide stopbands using only a few periods while avoiding all the challenges related

---

[a]Electronic address: adolph@chalmers.se

to the epitaxy of nitride-based DBRs. On the other hand, it requires extreme precision in the lift-off related processes making it challenging to fabricate cavities with a well-defined thickness. To achieve electrical injection, both approaches require intricate processing steps to define effective intra-cavity electrical paths since none of the employed DBR structures are electrically conducting.

We propose using ZnO/GaN DBRs for the formation of the optical cavity. This choice offers several advantages. The lattice-mismatch between ZnO and GaN is 1.9% which is comparatively small and therefore minimizes the risk of forming cracks. The difference between ZnO and GaN refractive indices is $\approx$0.4 at a wavelength λ of 450 nm. This difference is relatively large and means that a smaller number of periods (N < 20) are needed to achieve a high-reflectance DBR. Finally, n-doping of both ZnO[14] and GaN is straightforward meaning that an electrically conducting ZnO/GaN DBR can be achieved.

In this letter we report on the growth of ZnO/GaN DBRs by hybrid plasma-assisted molecular beam epitaxy (PAMBE) where both the ZnO and the GaN layers were grown in the same growth chamber.[15–18] This is the first time this type of structure has been reported. The DBR structures were deposited on GaN(0001)/Al$_2$O$_3$ templates and growth along both ZnO(0001) and ZnO(000$\bar{1}$) was investigated. We have earlier described the sample preparation and growth of smooth ZnO(0001), ZnO(000$\bar{1}$), and GaN(0001) using a combined oxide and nitride MBE-system.[17,18] The DBR stop-band center wavelengths were located between 400 and 500 nm. The highest reflectance achieved was 77% and was obtained for a 20-period DBR structure. All samples were free of cracks as revealed by optical microscopy and scanning electron microscopy (SEM).

Two ZnO/GaN DBR sample series, S1 and S2, were fabricated corresponding to two different growth approaches. The samples in S1 were grown along the ZnO(000$\bar{1}$) direction while the S2 DBRs were grown along the opposite ZnO(0001) direction. The ZnO-polarity was determined with HCl-wet etching.[18] All structures were initiated with the growth of a ZnO layer and concluded with a top GaN layer. The GaN-polarity of the top GaN layer was assessed using boiling KOH as described in Ref. 19. The S1 DBRs did not exhibit Ga-polar GaN (N-polar or mixed) whereas the GaN of the S2 DBRs was purely Ga-polar GaN. The determined polarity for GaN-layers grown on both ZnO(0001) and ZnO(000$\bar{1}$) is thus consistent with earlier reports.[19–21]

The S1 DBRs [along ZnO(000$\bar{1}$)] were grown with the O-plasma source RF power set to 300 W and with an O$_2$ flow rate Φ_{O_2} of 2.0 standard cubic centimeters (sccm) whereas the S2 DBRs [along ZnO(0001)] were grown with Φ_{O_2} = 1.0 sccm. The Zn beam equivalent pressure (BEP) was measured and adjusted to 0.8–1.0×10^{-6} Torr before each DBR growth.

The growth of the S1 samples was initiated with a 5 min O-plasma pre-exposure of the GaN/Al$_2$O$_3$(0001) templates with Φ_{O_2} = 2.0 sccm before opening the Zn-shutter.[18] All S1 ZnO layers were grown at a substrate growth temperature T_S of 350 °C. For most samples, we used the same T_S also for the GaN growth. A few S1 DBRs were grown with a 3–9 nm thick low-temperature (LT) GaN buffer layer at T_S = 350 °C followed by a high-temperature (HT) GaN layer grown at T_S = 650 °C corresponding to one pair of ZnO/(LT-GaN/HT-GaN). The Ga BEP was adjusted to 1.1–1.2×10^{-6} Torr before the growth of each S1 sample. All GaN layers were grown with the N-plasma source RF-power set to 250 W and with a N$_2$ flow rate Φ_{N_2} = 0.5 sccm.

The S2 DBR samples were grown with a LT and a HT step for both the ZnO and the GaN layers. One period of the S2 samples therefore corresponded to (LT-ZnO/HT-ZnO)/(LT-GaN/HT-GaN). It was not possible to achieve a smooth HT-GaN layer without a LT-GaN step. The LT-ZnO was grown at T_S = 300 °C before increasing to T_S = 450–500 °C for the deposition of the HT-ZnO layer. The corresponding values for LT- and HT-GaN were T_S = 450–500 °C and T_S = 630–650 °C, respectively. The T_S for the HT-ZnO and the LT-GaN was thus the same. We initiated each LT-ZnO growth with a 3 s pre-deposition of Zn on the GaN/Al$_2$O$_3$ (0001) templates at T_S = 300 °C before opening the shutter to the O-plasma. Once the LT-ZnO layer was completed, the T_S was increased under O-plasma exposure of the sample to the growth temperature for HT-ZnO. The deposition of the LT-GaN layers was initiated within 2–3 min after first switching off the O-plasma and then by simultaneously opening the shutters to the N-plasma source and the Ga source. The LT-GaN layers were 3–9 nm thick and were exposed to the N-plasma source during the temperature ramp up to the HT-GaN growth temperature.

TABLE I. Summary of selected properties for S1 and S2 ZnO/GaN DBRs. Listed is the number of periods N, the peak reflectance R, the stopband center wavelength λ_{SB}, the RMS roughness, and the PV distance as determined from AFM scans over $2 \times 2 \ \mu m^2$.

Sample	N	R (%)	λ_{SB} (nm)	RMS (nm)	PV (nm)
S1A	5	63	427	15.3	110
S1B	7	63	455	10.6	81.7
S1C	20	77	500	12.5	104
S2A	5	49/49	457/609	1.4	12.9
S2B	5.5	23/40	449/564	2.1	20.6

The absence of cracks was determined by inspection with an Olympus BX51 differential interference-contrast optical microscope. The surface morphology was characterized with both an Ultra 55 FEG SEM and a Bruker Dimension 3100 atomic force microscope (AFM) operated in tapping mode with a Si cantilever. The layer thickness was verified from cross-sectional SEM micrographs of the cleaved sample edge. A Filmetrics reflectometer was used to measure the reflectance spectra of the DBRs. We obtained x-ray diffraction (XRD) reciprocal space maps (RSMs) for the $(10\bar{1}5)$ reflection to determine the strain state of the samples. The XRD measurements were performed with a Panalytical X'Pert PRO MRD four-circle triple-axis diffractometer equipped with a $Cu_{K\alpha_1}$ source in the focus of a Ge(220) hybrid monochromator and a PIXcel-detector. The morphology and crystal structure of the layers were investigated with a Jeol 3000F transmission electron microscope (TEM) equipped with a field emission gun (FEG) and operating at 300 kV. Cross-sectional TEM lamellae were prepared with a FEI Nova NanoLab 600 DualBeam focused ion beam (FIB)/SEM system. A selected set of properties for the samples presented in this work is given in Table I. The samples have been grouped according to the S1 and S2 growth approach. The number of periods N is listed as well as the peak reflectance R, the stopband center wavelength λ_{SB}, the root-mean-square (RMS) roughness, and the peak-to-valley (PV) distance as determined from AFM scans over $2 \times 2 \ \mu m^2$.

Figure 1 shows an optical microscopy image of a 20-period DBR (sample S1C). The surface was free of cracks over the entire sample.

Figure 2(a) shows an SEM micrograph of the surface of a 5-period ZnO/GaN S1 sample DBR and (b) the surface of a 5-period S2 DBR. The surface morphology of the S1 sample was considerably rougher compared to the S2 DBR sample which had a virtually featureless surface. This was also confirmed by AFM which showed that the RMS roughness was 6–7 times larger for the S1 samples compared to the S2 DBR structures. The PV distance was ≈ 5 times larger (Table I). The RHEED-pattern from the first DBR pair was streaky for both S1 and S2 DBRs that included a HT- and LT-GaN layer. The next grown S1 DBR ZnO$(000\bar{1})$ layer exhibited a spotty RHEED pattern whereas the RHEED pattern for the S2 DBRs always remained streaky (except during the LT-GaN step). The increasing surface roughness for an increasing number of grown S1-DBR pairs is attributed to the difficulty to grow smooth ZnO$(000\bar{1})$ on non-Ga-polar GaN. The GaN layers in the S2 DBRs were single polar GaN(0001) only which improved the surface morphology. Nevertheless,
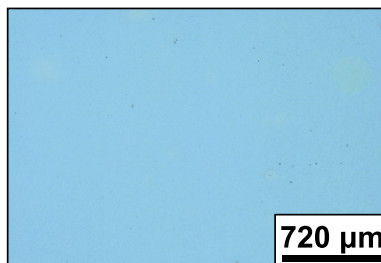

FIG. 1. Optical microscopy image of a crack-free 20-period ZnO/GaN DBR grown along the $(000\bar{1})$ direction (sample S1C).
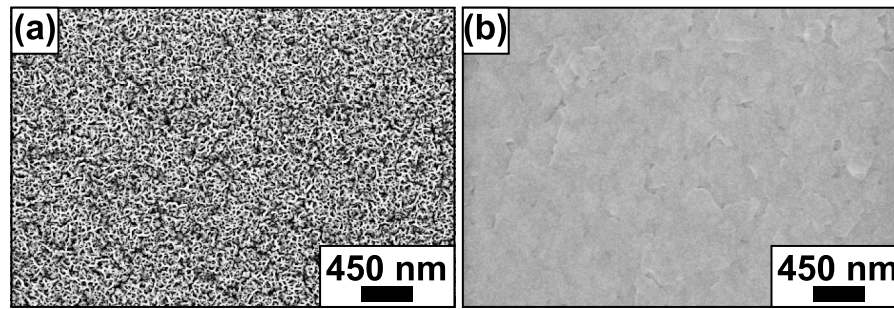
FIG. 2. SEM micrograph of the surface of (a) a 5-period ZnO/GaN DBR sample grown along $(000\bar{1})$ and (b) the surface of a 5-period DBR grown along the (0001) direction.

growth of GaN(0001) on ZnO($000\bar{1}$) has been reported showing that it could be possible to fabricate an S1 DBR with a smooth surface and interfaces.[19,20,22]

Figure 3 shows the reflectance spectra for both DBR sample series (S1 and S2). The maximum reflectance was obtained for the O-polar 20-period sample S1C which exhibited an R = 77%
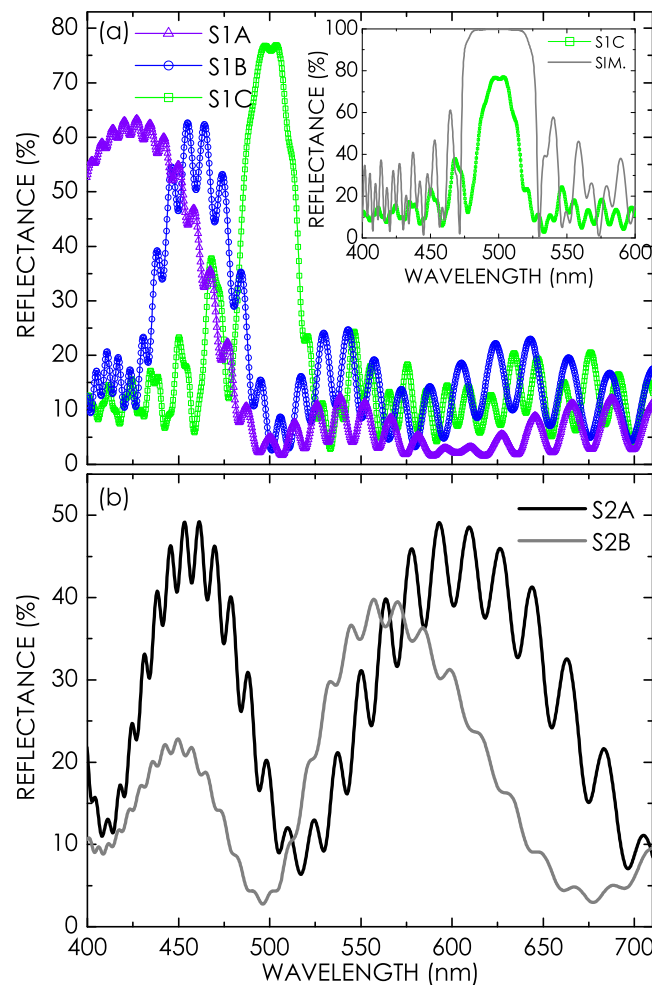

FIG. 3. (a) Reflectance spectra for the ZnO/GaN DBRs grown along the $(000\bar{1})$ direction (S1 series) and (b) reflectance for the DBRs grown along the opposite (0001) direction. The sample names are indicated. The inset in (a) shows a comparison between a simulation and the measured values for sample S1C.

with a stopband width of 32 nm centered at λ_{SB} = 500 nm [Fig 3(a)]. This stopband position corresponds to a ZnO layer thickness of 60.9 nm and a GaN thickness of 51.0 nm according to the $\lambda/4$ criteria. The DBR samples with lower number of periods showed a lower reflectance, as expected. The sample S1A DBR with N = 5 was grown with a LT/HT-GaN structure according to ZnO/(LT-GaN/HT-GaN). This sample exhibited a R = 63% which was the same reflectance obtained for sample S1B grown with N = 7 and with the same low growth temperature for both ZnO and GaN (T_S = 350 °C). This indicates that the LT/HT-GaN method improved the reflectance due to an improved interface quality for the ZnO/(LT-GaN/HT-GaN) structure (sample S1A).

The reflectance spectra for the samples grown along the (0001) direction (S2 samples) showed multiple reflectance peaks [Fig. 3(b)]. This was caused by a failing Zn-source resulting in an uncontrollable Zn-flux. Through the course of the growth, the ZnO layer thickness therefore varied which was also later verified by SEM. These samples also exhibited Ga-droplets on the surface indicating Ga-rich growth conditions during the deposition of the GaN layers. The residual Ga resulted in thicker GaN layers since the N-plasma source was on during the temperature ramps before and after the growth of the HT-GaN layer. We found that Ga-rich or Ga-stable conditions were necessary for achieving a smooth surface morphology since experiments with N-rich growth resulted in a plateau-valley morphology. Ga-stable conditions are preferred since an accurate layer thickness and a droplet-free surface are achieved.

The inset in Fig. 3(a) shows a comparison between a simulation of the reflectance of sample S1C and the experimental values. The simulation was based on the transfer matrix method. The Sellmeier equation from Ref. 23 based on the data in Ref. 24 was used to calculate the dispersion of the ZnO refractive index. Ellipsometric measurements of thick GaN films were used to extract the corresponding dispersion relation. We believe that the large discrepancy observed between simulation and experiment was caused by the rough surface morphology [Table I and Fig. 2] in conjunction with inhomogeneous interfaces for this and other S1 samples. The pronounced interference fringes of sample S2A in Fig. 3(b) and the relatively high reflectance compared to the S1A and S1B samples despite the varying layer thicknesses indicate that the interface quality is higher than the DBRs grown along the (000$\bar{1}$) direction.

Figure 4 shows micrographs from high-angle annular dark-field scanning TEM (HAADF-STEM), conventional TEM, and high-resolution TEM (HRTEM) micrographs as well as the corresponding fast-Fourier transform (FFT) power spectra of sample S1 [Figures 4(a)–4(c)] and S2 [Figures 4(d)–4(f)].

The periodic ZnO/GaN structure can be observed clearly in Fig. 4(a). The individual ZnO (dark) and GaN (bright) layers are indicated in this figure. In Fig. 4(b) the layers can be distinguished by the phase contrast. Figure 4(c) shows a magnified zone of a GaN/ZnO pair. The additional reflections in the FFT power spectrum of the inset in Fig. 4(c) are caused by twin defects in the ZnO layer. As the ZnO layers of the second sample are thin, these reflections do not appear in the power spectrum in Fig. 4(f).

Figure 5(a) shows RSMs across the (10$\bar{1}$5) reflection for (a) the 20-period sample S1C ZnO/GaN DBR and (b) the 5.5-period sample S2B DBR, respectively. The dashed line indicates the position of the GaN reflection. The slightly differently shaped contours of the RSMs are an artifact of the PIXcel-detector setting. The weak ZnO(10$\bar{1}$5) diffraction peak in Fig. 5(a) is located to the lower left with respect to GaN(10$\bar{1}$5). We calculated the corresponding in-plane ZnO lattice constant a_{ZnO} to 0.324 nm which is close to the bulk ZnO lattice constant $a_{ZnO,bulk}$ of 0.325 nm. Our layer was thus almost completely relaxed (76%–88% with respect to GaN). The GaN layer was assumed to be completely relaxed in this assessment. The absence of a contour tail between the peaks indicates that the relaxation was abrupt. In contrast, the diffraction peak for the 5.5-period-S2B DBR is located on the dashed line meaning that the in-plane ZnO and GaN lattice constants are equal. The ZnO layers are therefore strained or possibly the whole DBR structure has approached a strain-compensated state with a minimum net residual strain. The different strain-states between these two structures must be caused by a fundamental difference between the corresponding growth methods [growth along (000$\bar{1}$) vs. (0001)] or an abrupt relaxation process occurring after 5.5 periods.
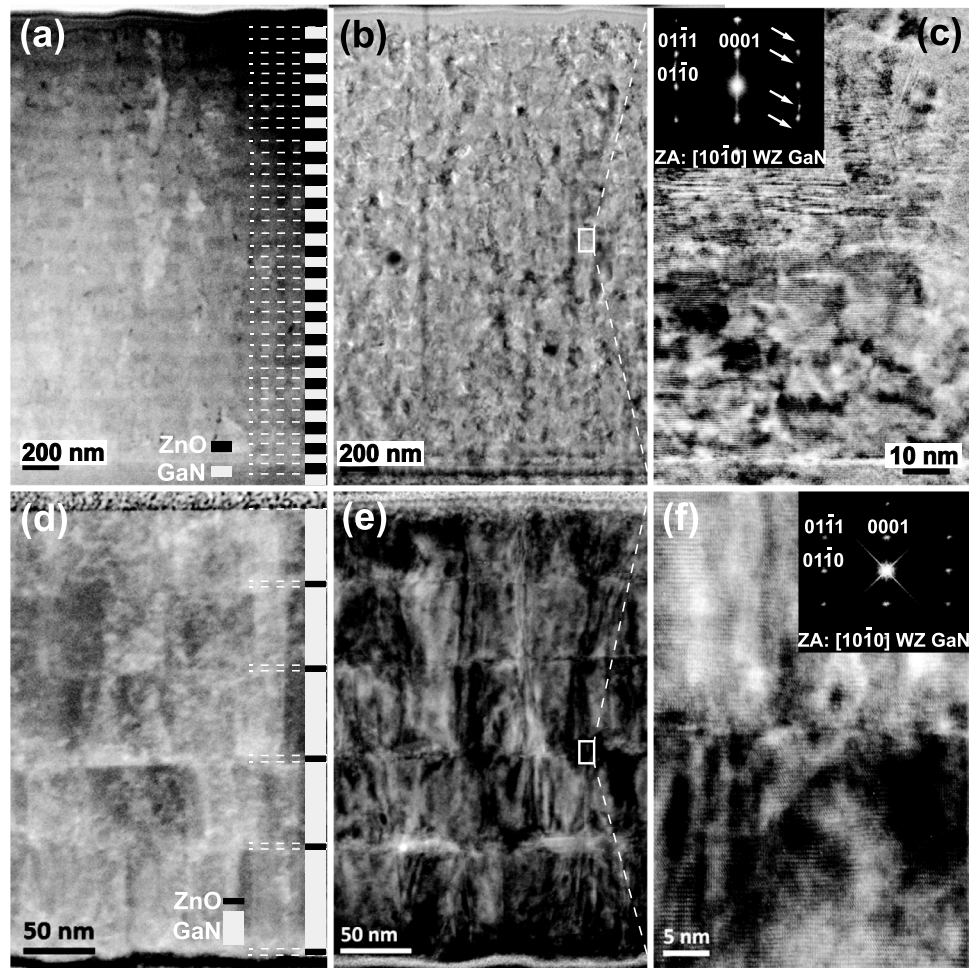
FIG. 4. ((a)-(c)) Cross-sectional TEM analysis of a 20-period ZnO/GaN DBR (sample S1C) and ((d)-(f)) of a 5-period DBR (sample S2A). (a) and (d) HAADF-STEM phase contrast images and (b) and (e) TEM phase contrast images. (c) HRTEM image of the 20-period ZnO/GaN structure. The additional power spectrum reflections shown in the inset (indicated with arrows) reveal that the ZnO layer contains several twin boundaries. (f) HRTEM image of the 5-period ZnO/GaN structure. No additional reflections can be observed since the ZnO layers are very thin.

Our ZnO layers have a background electron concentration of 1×10^{19} cm^{-3}. The corresponding value for the GaN layers is 1.8×10^{18} cm^{-3}.[17] Controlled n-doping of ZnO has been reported[14] and n-doping of GaN with Si is straightforward. In addition, ZnO transparent contacts to GaN-based light-emitting diodes have been demonstrated.[25,26] Since both ZnO and GaN exhibit n-type conductivity and transparent ZnO contacts to GaN LEDs have been demonstrated, the reported ZnO/GaN DBRs could be a possible route for vertically conducting n-type DBRs.

To summarize, we have demonstrated novel ZnO/GaN DBRs where the complete structure was grown in-situ (without exposure to air between layers) using the same growth chamber for both ZnO and GaN. Growth along both ZnO(0001) and ZnO(000$\bar{1}$) was investigated. The DBRs were crack-free and consisted of up to 20 periods. The maximum achieved reflectance was 77% at a stopband center wavelength of 500 nm. Growth along ZnO(0001) yielded smoother layers and more abrupt interfaces than growth along ZnO(000$\bar{1}$). Based on our results, it should be possible to grow a cavity structure consisting of a conducting ZnO/GaN DBR and an active region, completely in-situ.
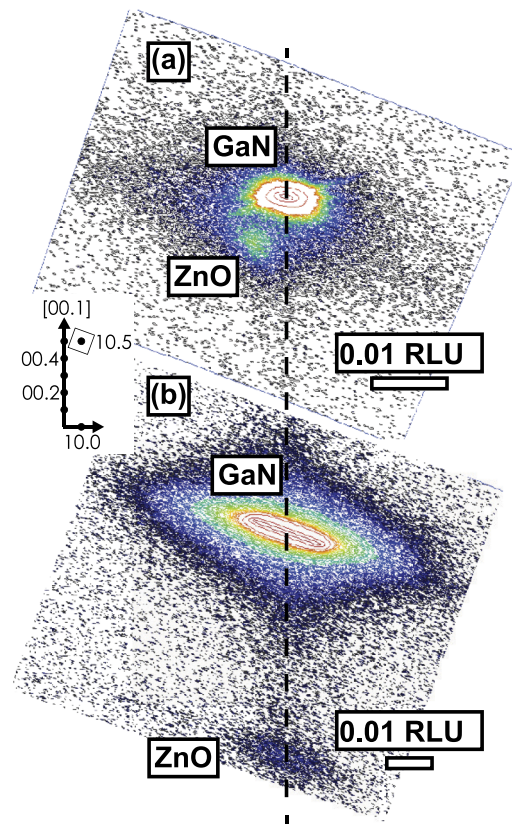
FIG. 5. Reciprocal space maps for the asymmetric (10$\bar{1}$5) reflection of (a) a 20-period ZnO/GaN DBR (sample S1C) and (b) a 5.5-period DBR (sample S2B). The vertical dashed line indicates the position of the GaN(10$\bar{1}$5) reflection.

[1] Y. Higuchi, K. Omae, H. Matsumura, and T. Mukai, Appl. Phys. Express **1**, 121102 (2008).

[2] T.-C. Lu, C.-C. Kao, H.-C. Kuo, G.-S. Huang, and S.-C. Wang, Appl. Phys. Lett. **92**, 141102 (2008).

[3] G. Cosendey, A. Castiglia, G. Rossbach, J.-F. Carlin, and N. Grandjean, Appl. Phys. Lett. **101**, 151113 (2012).

[4] W.-J. Liu, X.-L. Hu, L.-Y. Ying, J.-Y. Zhang, and B.-P. Zhang, Appl. Phys. Lett. **104**, 251116 (2014).

[5] C. O. Holder, J. S. Speck, S. P. DenBaars, S. Nakamura, and D. Feezell, Appl. Phys. Express **5**, 092104 (2012).

[6] T. Onishi, O. Imafuji, K. Nagamatsu, M. Kawaguchi, K. Yamanaka, and S. Takigawa, IEEE J. Quantum Electron. **48**, 1107 (2012).

[7] T.-C. Lu, J.-R. Chen, S.-W. Chen, H.-C. Kuo, C.-C. Kuo, C.-C. Lee, and S.-C. Wang, IEEE J. Sel. Top. Quantum Electron. **15**, 850 (2009).

[8] T.-C. Lu, T.-T. Wu, S.-W. Chen, P.-M. Tu, Z.-Y. Li, C.-K. Chen, C.-H. Chen, H.-C. Kuo, and S.-C. Wang, IEEE J. Sel. Top. Quantum Electron. **17**, 1594 (2011).

[9] T.-C. Lu, S.-W. Chen, T.-T. Wu, P.-M. Tu, C.-K. Chen, C.-H. Chen, Z.-Y. Li, H.-C. Kuo, and S.-C. Wang, Appl. Phys. Lett. **97**, 071114 (2010).

[10] K. Omae, Y. Higuchi, K. Nakagawa, H. Matsumura, and T. Mukai, Appl. Phys. Express **2**, 052101 (2009).

[11] D. Kasahara, D. Morita, T. Kosugi, K. Nakagawa, J. Kawamata, Y. Higuchi, H. Matsumura, and T. Mukai, Appl. Phys. Express **4**, 072103 (2011).

[12] C. O. Holder, J. T. Leonard, R. M. Farrell, D. A. Cohen, B. Yonkee, J. S. Speck, S. P. DenBaars, S. Nakamura, and D. F. Feezell, Appl. Phys. Lett. **105**, 031111 (2014).

[13] J. T. Leonard, D. A. Cohen, B. P. Yonkee, R. M. Farrell, T. Margalith, S. Lee, S. P. DenBaars, J. S. Speck, and S. Nakamura, Appl. Phys. Lett. **107**, 011102 (2015).

[14] T. Ben-Yaacov, T. Ive, C. G. Van de Walle, U. K. Mishra, J. S. Speck, and S. P. Denbaars, J. Electron. Mater. **39**, 608 (2010).

[15] M. Johnson, S. Fujita, W. Rowland, W. Hughes, J. Cook, and J. Schetzina, J. Electron. Mater. **25**, 855 (1996).

[16] D. Adolph and T. Ive, Appl. Surf. Sci. **307**, 438 (2014).

[17] D. Adolph, T. Tingberg, and T. Ive, J. Cryst. Growth **426**, 129 (2015).

[18] D. Adolph and T. Ive, Phys. Status Solidi (b) **253**, 1523–1528 (2016).

[19] Y. Xia, J. Brault, P. Vennègués, M. Nemoz, M. Teisseire, M. Leroux, and J.-M. Chauveau, J. Cryst. Growth **388**, 35 (2014).

[20] X. Gu, M. A. Reshchikov, A. Teke, D. Johnstone, H. Morkoç, B. Nemeth, and J. Nause, Appl. Phys. Lett **84**, 2268 (2004).

[21] G. Namkoong, S. Burnham, K.-K. Lee, E. Trybus, W. A. Doolittle, M. Losurdo, P. Capezzuto, G. Bruno, B. Nemeth, and J. Nause, Appl. Phys. Lett **87**, 184104 (2005).

[22] A. Kobayashi, Y. Kawaguchi, J. Ohta, H. Fujioka, K. Fujiwara, and A. Ishii, Appl. Phys. Lett **88**, 181907 (2006).

[23] Optical Society of America, *Handbook of Optics*, 3rd ed. (McGraw-Hill, 2009), Vol. 4.

[24] W. L. Bond, J. Appl. Phys. **36**, 1674 (1965).

[25] T. Ive, T. Ben-Yaacov, H. Asamizu, C. G. V. de Walle, U. Mishra, S. P. DenBaars, and J. S. Speck, Phys. Status Solidi (C) **5**, 1733 (2008).

[26] T. Ive, T. Ben-Yaacov, A. Murai, H. Asamizu, C. G. V. de Walle, U. Mishra, S. P. DenBaars, and J. S. Speck, Phys. Status Solidi (C) **5**, 3091 (2008).